COMPUTER SIMULATION OF OFFSET PRINTING: I. EFFECTS OF IMAGE COVERAGE AND INK FEEDRATE

Shem M. Chou* and Lawrence J. Bain*.

Keywords: Lithography, Simulation, Image Coverage, Ink Feedrate, Dynamics

Abstract: A computer program was written in QuickBASIC to simulate printing process of a web offset press in both 100-0-0 and 60-20-20 inker configurations. Printed ink film thickness, rates of ink flowing through each of the three ink form rollers and to the web, and quantity of ink built up in the inker all were found to follow a first order differential equation for step changes in ink feedrate, from which the press time constant and incubation period are derived. The simulation results indicate that based on the ink film thickness measurement both press time constant and incubation period are independent of any change in ink feedrate, whether it is a stop increase or decrease and whether it is a large or small change. This finding appears to contradict results reported in the literature. However, if the optical density measurement is used as a process control means, the press needs a longer time to respond to a step decrease in ink feedrate than to a step increase, due to the non-linear relationship between ink film thickness. and optical density. It was also found that the press time constant and mean ink residence time are inversely proportional to the image coverage. These findings and inker configuration effect on dynamic characteristics of press and uniformity of printed ink films are presented. Applications of press simulation to closed-loop control of the printing process are also discussed.

Introduction

Lithography is the most popular but yet the most complicated printing process. It is full of challenges to both academic and industrial researchers. In addition to the delicate ink-water balance, the number of inking rollers in a lithographic press is much larger than that of a gravuer or flexographic press. Each printing couple generally consists of up to about ten rollers including two ink form rollers for a newspaper press,

Rockwell Graphic Systems, 700 Oakmont Lane, Westmont, IL 60559
Tel: (708) 850-6461, E-mail: smchou@graphics.rockwell.com

more than ten rollers including three ink form rollers for a commercial web press, and more than twenty rollers including four ink form rollers for a sheetfed press. In comparison, a gravure or flexographic press has only a couple of inking rollers. It is a general perception in the printing industry that the more ink form rollers in a lithographic press, the higher the print quality. However, this intuitional perception remains to be proven.

It is not only costly but also impractical to experiment with all possible roller arrangements of an inker in the development of a new printing press and to run a press for assessing its performance. Computer simulation has been applied in many industries as a cost-effective and time-efficient way of developing a very complicated system. Many attempts were made in the past to model the ink distribution process of a printing press to calculate the thickness of ink films on the substrate and on inking roller surfaces. The uniformity of ink film thickness on a substrate and the dynamic response of the press to a change in ink or fountain solution feedrate are the two primary criteria for assessing press performance. The former is related to print quality and the latter to the waste resulting from the makeready and a change in ink or water feedrate. This study will demonstrate that computer simulation of printing process is a very powerful tool for assessing performance of existing presses, developing new press designs, and studying press dynamics for process control.

Variations of ink film thickness normally result from improper setting of ink fountain keys. However, there are two image-related variations of ink film thickness that cannot be compensated by ink key adjustment. They are ghost and starvation. When ink is transferred from an ink form roller to the plate, a memory of printed image resides on that roller, which subsequently propagates to the other inking rollers and fades rapidly further away from the plate cylinder. Because the diameters of ink form rollers are generally smaller than that of plate cylinder, this image memory on the ink form roller overlaps with another part of the plate image, resulting in the so-called ghost. The gap in the plate cylinder can also cause a variation of ink film thickness in a way similar to ghost. So, ghosts is an ink film thickness variation in the printing direction and in most cases can be concealed with a proper layout of images. It can be eliminated completely, if the size of ink form roller is the same as that of plate cylinder. However, this concept is not popular in the industry.

In lithographic printing, the ink fountain keys are generally regulated according to the image format so that the feedrate of ink in any inking zone is equal to the rate of ink taken away by the printing substrate of that zone. All lithographic printing presses are equipped with a number of vibrators to prevent the formation of ridges, which adversely causes a lateral flow of ink from high to low image-coverage zones. When there are abrupt changes in the image coverage across the press, the lateral flow of ink becomes so significant that the print density of low coverage images is higher than the target value and that of high coverage is lower. This difference in the print density is generally referred to as starvation. So, starvation is an ink film thickness variation in the cross-press direction and in most cases can be concealed with a proper layout of

images. If the abrupt change in the image coverage happens to occur in a particular inking zone, it is impossible to eliminate the starvation. Press manufacturers are more interested in designing an inker with a minimal effect on starvation.

Mill (1961), Hull (1968), and Guerrette (1985) calculated the steady-state ink film thickness distribution by solving a set of simultaneous continuity equations for a particular inking system The average ink film thicknesses before and after transfer are calculated as a function of image coverage of the plate. Implementation of these methods is relatively simple, though. The effect of image layout on the ink film thickness distribution is neglected. Ghost is assumed to reduce by one half each time the image memory passes through a roller nip (Hull, 1968 and Guerrette, 1985).

In the approach taken by Scheuter and Rech (1970) and MacPhee (1995), the circumferences of inking rollers are divided into many segments of equal length. All of the rollers rotate one segment at a time during printing and the ink film thickness on each segment emerging from the roller nip is calculated. This one-dimensional computer simulation involves tremendous mathematical calculations and is much more time-consuming than the method of solving simultaneous equations. However, it is possible to calculate the actual ghost caused by the improper image layout and the gap in the plate cylinder. The dynamic behavior of inking systems can also be predicted.

The aforementioned computer simulations do not take into account the lateral flow of ink caused by the oscillation of vibrators. Quantitative prediction of starvation is not possible. In this study the one-dimensional computer simulation is extended to two-dimensional, that is, the variations of ink film thickness in both printing and cross-press directions are calculated. This paper focuses on the dynamic behavior of lithographic presses. The simulation results of print quality attributes such as ghost and starvation are presented elsewhere (Chou, et al., 1996).

Computer Simulation Methodology

The Hantscho World 16 press manufactured by Rockwell Graphic Systems is an ideal candidate for computer simulation. The inker can be toggled between 100-0-0 and 60-20-20 roller configurations by throwing the bridge roller (BR) off (dotted circle) or on (solid circle), as shown schematically in Figure 1. This allows a direct comparison of press performance between the two roller configurations.

In the computer simulation, the surfaces of all inking rollers and plate and blanket cylinders are divided into many small cells of the same size, as shown schematically in Figure 2. The size of cells is determined by the desired image resolution, computer resources and simulation time. For example, if each cell is subdivided into 4 cells (2 by 2), the resolution is quadrupled. The number of calculations, the size of computer memory needed to store ink film thickness information, and the, time spent in running the simulation program are also quadrupled. These factors have to be compromised when planning the computer simulation program. The number of cells between two

WORLD 16 PRESS

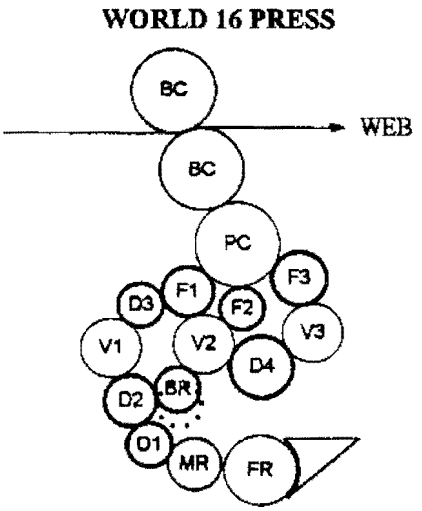

Figure 1. Schematic diagram illustrating the roller configuration of a Hantscho World 16 press used in the computer simulation.

adjacent roller nips in the printing direction has to be rounded off to the nearest whole number. The number of cells in the cross-press direction is also rounded off to the nearest whole number. The cell size selected in this study is 0.25" by 0.25". There are 91 cells around the press cylinder and 140 cells across the press for a 35" web. It took more than 8 hours to run a simulation of 520 plate cylinder revolutions on a Dell OptiPlex XMT 590 computer.

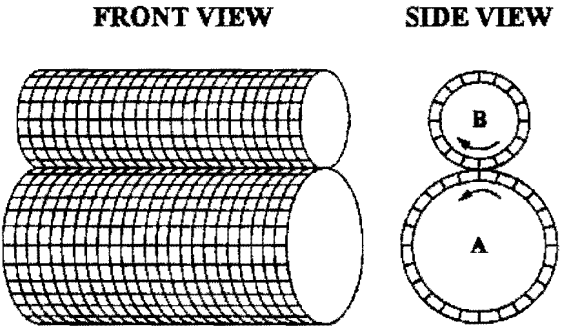

Figure 2. Schematic diagram showing the roller surfaces divided into many small cells of the same size. Each cell contains ink film thickness information.

To simplify the computer simulation, the following assumptions were made.

1. There is no squeeze flow of ink in any direction in the roller nips.
2. There is no roller slippage and ink piling in the nip entrance.
3. The film splitting is smooth and no ink is lost from the interacting cells.
4. All the rollers rotate simultaneously one cell in the printing direction in each time interval.
5. The vibrators are silenced.
6. The effect of fountain solution on ink transfer is ignored.

The first three assumptions are required for the conservation of ink volume involved in ink distribution That is, the inflow of ink to two interacting cells is the same as the outflow. The assumption of no squeeze flow is needed to neglect the dot gain. The effect of oscillation of vibrators on press performance will be discussed in the second papa of this series. Fountain solution complicates tremendously the simulation of printing process. It will be included in the simulation program in the future, when we can quantify more precisely the distribution of water in the inker and water evaporation.

The ink film thicknesses at the exit of any inking roller nip, e.g. ink distribution from Rollers A to Roller B in Figure 2, can be expressed by the following equations:

$$H'_B(i,j) = S_{AB}\left[H_A(k,j) + H_B(i,j)\right] \tag{1}$$

and

$$H'_A(k,j) = (1 - S_{AB})\left[H_A(k,j) + H_B(i,j)\right] \tag{2}$$

where H_A, H_B, H_A`, and H_B' are the inflow and outflow ink film thicknesses on Rollers A and B, respectively. The indices (i, j) and (k, j) specify the cells involved in ink distribution. The first and second indices indicate respectively the cell positions in the printing and cross-press directions. Because the oscillation of vibrators is not considered in this paper, the same index j is used. The split ratio, S_{AB}, is the fraction of ink in the roller nip that is distributed to Roller B.

For nips involving an ink form roller and the plate cylinder, the fractional image coverage of each cell on the plate cylinder has to be included in the distribution equations as follows.

$$H'_P(i,j) = S_{FP}\left[H_P(i,j) + H_F(k,j)\right] \tag{3}$$

and

$$H'_F(k,j) = F(i,j)(1 - S_{FP})\left[H_P(i,j) + H_F(k,j)\right] + \left[1 - F(i,j)\right]H_F(k,j) \tag{4}$$

where the subscripts F and P represent ink form roller and plate cylinder, respectively.

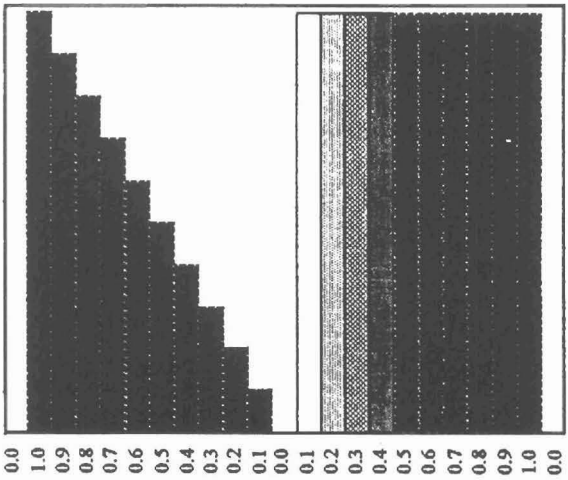

Figure 3. Bar graph used as the test form in this computer simulation to study the dynamic behavior of the inking systems.

F(i, j) is the fractional image coverage of cell P(i, j) on the plate cylinder. Eq. (3) which is identical to Eq. (1), is included here for a complete expression of ink distribution between ink form roller and plate cylinder. In fact, Eqs. (1) to (4) are the same as those reported by Guerrette (1985). All the split ratios are assumed to be 0.5 in this study.

The bar graph shown in Figure 3 was used as the test form to study the dynamic behavior of inking systems. The left and right pages of the bar graph test form consist of solid and halftone bars, respectively. The image coverages of those bars vary from 10% to 100% in an increment of 10%. The image coverage is indicated by the number under each bar. The width of each bar is equal to the width of an ink fountain key, and there are six cells across each bar. The ink feedrate from each key was set proportional to the image coverage of that printing zone. The simulation process, starting with a clean inker, included four stages of varying ink feedrate. The target thickness of ink film on the printing substrate was 1 μm in the first stage, increased to 1.5 μm in the second stage, brought back to I μm in the third stage, and the ink feed was completely terminated in the fourth stage. The press was allowed to run for 520 plate cylinder revolutions at each stage.

This computer simulation program allows us to monitor the ink film thickness printed on the substrate, rates of ink flowing through each of the three ink form rollers and to the web, and the—quantity of ink volume built up in the inker as a function of plate cylinder revolutions. Information about the ink film thickness distribution on the entire inker can also be saved for each plate cylinder revolution, as long as the disk storage space is not an issue. For example, the file size is 50K bytes for one printed sheet and 481K for the inker. That is, at least 1 giga-byte space is needed to store the ink film thickness data for one simulation of four inking stages.

Computer Simulation Results

Ink Flow Ratios

One of the characteristics for lithographic presses is the multiple ink form rollers. Each form roller contributes a portion of ink film to the plate and this fractional contribution is generally referred to as the ink flow ratio. Wirz (1964) observed experimentally that the ink flow ratios varied with inker configurations and the first ink form roller always contributed most of the ink to the plate. He did not investigate the relationship between ink flow ratio and print quality. Guerrette (1985) reported that the ink flow ratios also varied with the image coverage, and the first down inkers produced less ghosting than the second down inkers.

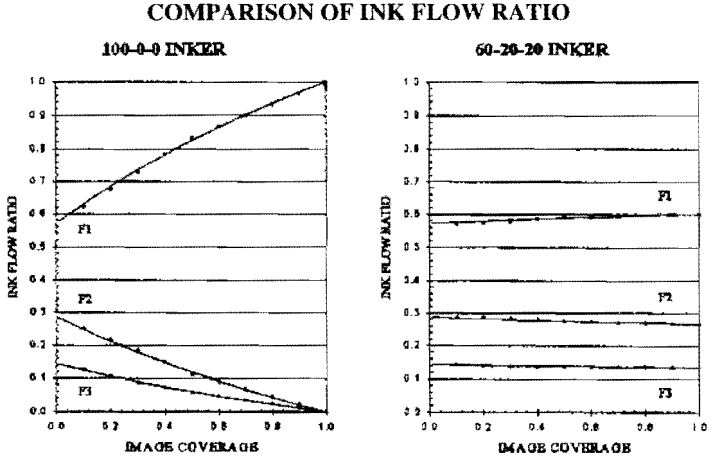

Figure 4. Ink flow ratios of the 100-0-0 and 60-20-20 inkers as a function of image coverage.

Figure 4 compares the ink flow ratio curves of the 100-0-0 and 60-20-20 inkers. The marks represent the data obtained from this study. The lines drawn through the data were obtained by solving the simultaneous continuity equations using the method proposed by Guerrette (1985). The results from both methods agree with each other very well. Both inkers have the same ink flow ratios at zero image coverage, but the discrepancy becomes larger and larger with increasing image coverage. For the 100-0-O inker, the ink flow ratio of the first form roller increases rapidly with the image coverage and approaches 0.997 at 100% coverage, while the ink flow ratios of the second and third form rollers decrease rapidly to 0.002 and 0.001, respectively. These numbers differ slightly from 1, 0, and 0 obtained by Guerrette's method. The difference can be attributed to the disturbance caused by the plate cylinder gap in the present simulation. For the 60-20-20 inker, the ink flow ratio of the first form roller increases slightly with the image coverage, while those of the second and third form rollers decrease very little. The ink flow ratios of the first, second, and third form rollers are respectively 0.600, 0.267, and 0.133 at 100% image coverage.

WORLD 16 PRESS/60-20-20 INKER
100% Solid Bar

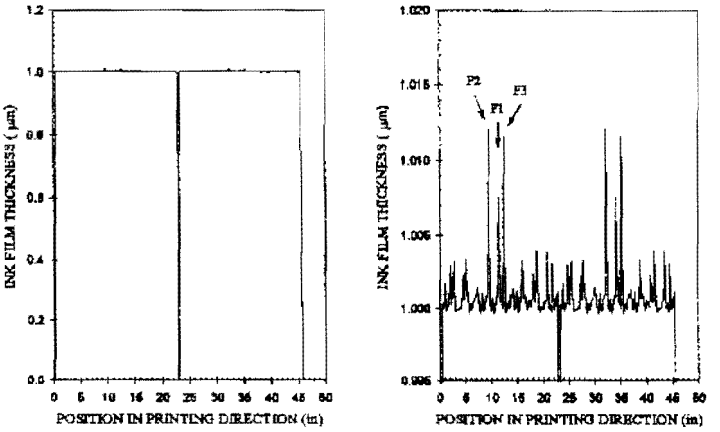

Figure 5. Ink film thickness profile of the 100%-coverage solid bar obtained from the 519th and 520th impressions of the 60-20-20 inker. The right chart is a close-up view of the left.

WORLD 16 PRESS/100-0-0 INKER
100% Solid Bar

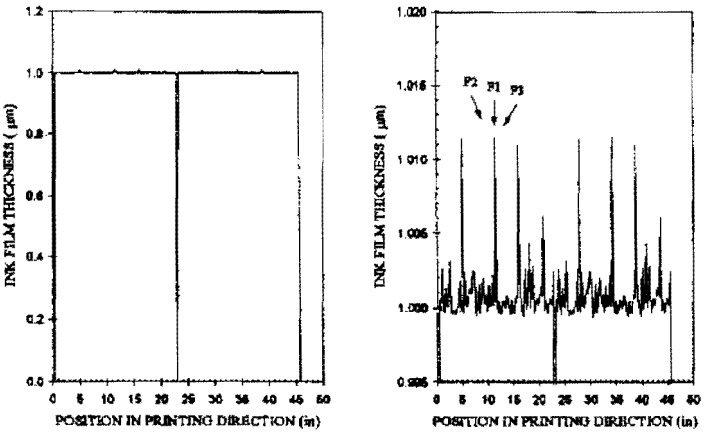

Figure 6. Ink film thickness profile of the 100%-coverage solid bar obtained from the 519th and 520th impressions of the 100-0-0 inker. The right chart is a close-up view of the left.

Uniformity of Ink Film Thickness

Uniformity of ink film thickness is the most important criterion for print quality. Figure 5 shows the ink film thickness profile of the solid bar with 100% image

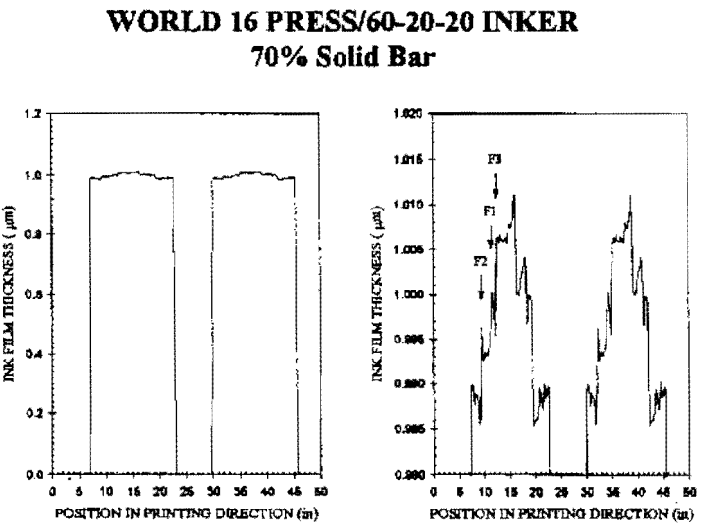

Figure 7. Ink film thickness profile of the 70%-coverage solid bar obtained from the 519th and 520th impressions of the 60-20-20 inker. The right chart is a close-up view of the left.

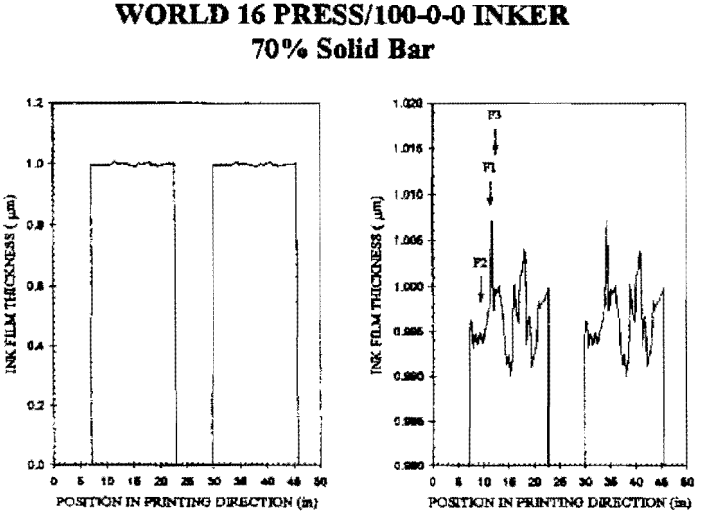

Figure 8. Ink film thickness profile of the 70%-coverage solid bar obtained from the 519th and 520th impressions of the 100-0-0 inker. The right chart is a close-up view of the left.

coverage obtained from the 519th and 520th impressions of the 60-20-20 inker. The close-up view shows three major peaks on each page corresponding to the principal ghosts of the plate cylinder gap produced by three form rollers, as indicated by F1, F2, and F3. Since the first ink form roller contributes 60% of ink to the plate, it is expected to produce the largest ghost. This ghost is attenuated by the subsequent two nips of plate cylinder with the second and third form rollers, and eventually becomes the smallest one. The second form roller contributes twice as much ink to the plate as the third one, but its ghost is attenuated by one nip more than that of the third form. The net result is that the magnitudes of ghost produced by the second and third forms are nearly the same.

Because the first form contributes almost all of the ink to the plate at 100% image coverage for the 100-0-0 inker, it is predicted that ghosts produced by the second and third form rollers do not exist. This is indeed the case as shown in Figure 6. It is noted, as compared to the close-up chart in Figure 5, that the magnitude of ghost from the first form roller is approximately the same as those produced by the second and third form rollers of 60-20-20 inker. These results indicate that the primary function of the second and third form rollers of the 100-0-0 inker is to smooth out the ink film on the plate. Two other major peaks also appear in the profile of the 100-0-0 inker. Their origin is not certain yet at the present stage.

Figures 7 and 8 show the ink film thickness profiles of the solid bar with 70% image coverage for the 60-20-20 and 100-0-0 inkers, respectively. Referring to the test form in Figure 3, the ghost of this solid bar comes from the plate cylinder gap and the non-image area in the leading edge. It is obvious that three principal ghosts overlap one

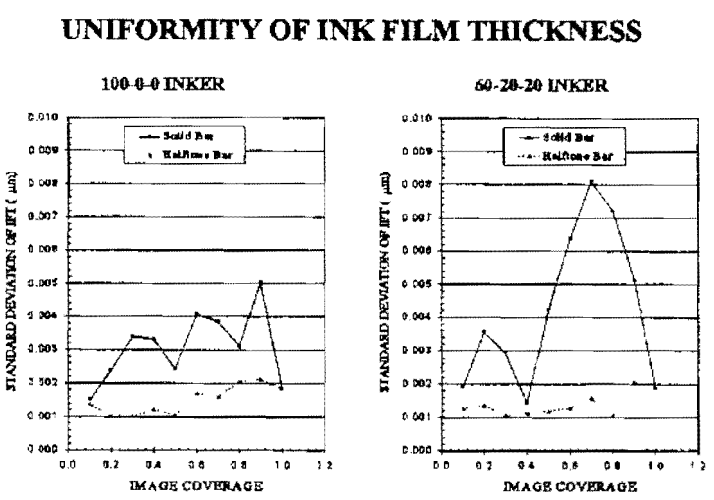

Figure 9. Standard deviation of ink film thickness as a function of image coverage for the solid and halftone bars produced by the 100-0-0 and 60-20-20 inkers.

another in the printed image of the 60-20-20 inker, whereas the ghost is attenuated by the second and third form rollers of the 100-0-0 inker. Thus, ink films produced by the 60-20-20 inker are predicted to be less uniform than those of the 100-0-0 inker. Figure 9 shows the standard deviation of ink film thickness as a function of image coverage. These results provide further evidence to support the prediction. They also show that the standard deviations of ink film thickness for the halftone bars are overall much smaller than those of solid bars, because the plate cylinder gap is the only source of ghosting in the latter case.

Dynamic Behavior

Figures 10 and 11 illustrate respectively the average printed ink film thicknesses of the 50% and 10% solid bars as a function of plate cylinder revolutions obtained from simulating the 100-0-0 inker. The solid lines are drawn according to the equation reported by Neuman and Almendinger (1978) as follows.

$$H = H_0 + (H_\infty - H_0)\,[1 - \exp[-(N - N_d)/\tau_p]] \qquad (5)$$

where H and N represent respectively the ink film thickness on the substrate and the number of plate cylinder revolutions. H_0 and H_d. are the initial and steady-state ink film thicknesses after a step change in ink feedrate. N_d is the incubation period or delay time which is the time elapsed before the output begins to respond to the stop change. Any change in ink feedrate at the ink fountain has to travel through all the inking rollers and the plate and blanket cylinders to become effective on the web. The incubation period thus results. The theoretical incubation periods for 100% image coverage are 2.49 and 2.81 plate cylinder revolutions for the 60-20-20 and 100-0-0 inkers, respectively. τ_p is the press time constant characterizing how fast the process reaches the steady state. For example, the inking system will achieve 63.2%, 95.0%, and 99.3% to the steady state after 1 τ_p, 3 τ_p, and 5 τ_p impressions, respectively.

The results in Figures 10 and 11 indicate that the dynamic behavior of lithographic printing process can be described very well by Eq. (5) at all four inking stages. Excellent agreement between theoretical predictions and simulation results was also obtained for other image coverages. Close examination of Figures 10 and 11 reveals that the ink film thickness of the 50% solid bar almost reaches the steady state at 200 plate cylinder revolutions, while that of the 10% solid bar is still far away from the steady state even at 520 revolutions. It appears that the printed ink film thickness approaches the steady state faster, the higher the image coverage. This tentative conclusion is confirmed by the data in Tables 1 and 2, which summarize the press time constant and incubation period characterizing the dynamic behavior of the 100-0-0 inker as a function of image coverage. Statistical data are also included. It is noted that both press time constants and incubation periods of all four stages for each image coverage are the same from the statistical viewpoint. Similar results were also obtained

from the halftone bars as well as from the 60-20-20 inker. These results indicate that both press time constant and incubation period are independent of any change in ink feedrate, whether it is a step increase or decrease and whether it is a large or small change.

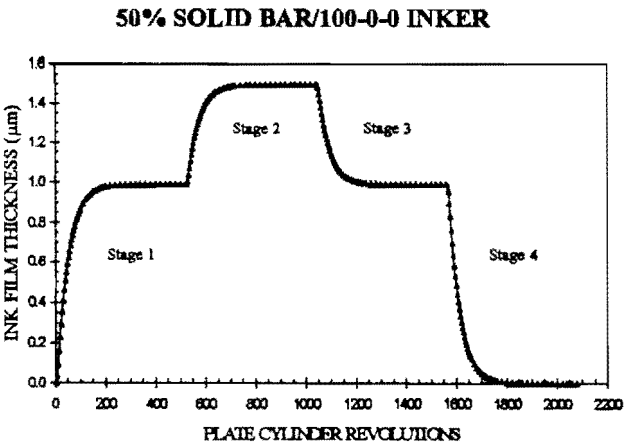

Figure 10. Dynamic behavior of printed ink film thickness of the 50% solid bar obtained from the computer simulation of the 100-0-0 inker.

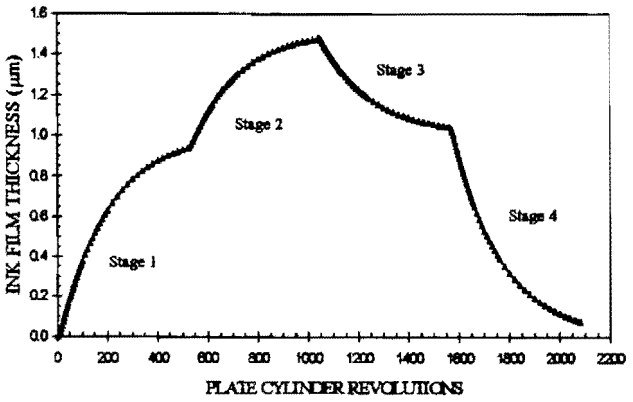

Figure 11. Dynamic behavior of printed ink film thickness of the 10% solid bar obtained from the computer simulation of the 100-0-0 inker.

The mean press time constant and the mean incubation period data in Tables 1 and 2 are plotted in Figure 12 to illustrate the effect of image coverage on dynamic behavior of the 100-0-0 inker. The press time constant is inversely proportional to the image

Table 1. Press time constant of solid bars as a function of image coverage obtained from simulating the 100-0-0 inker for all four inking stages.

Image Coverage	Stage of Ink Feed 1	2	3	4	Mean	Standard Deviation
0.1	195.68	195.52	195.75	195.64	195.65	0.086
0.2	100.68	100.67	100.69	100.68	100.68	0.006
0.3	69.40	69.39	69.40	69.40	69.40	0.001
0.4	53.84	53.84	53.84	53.84	53.84	0.001
0.5	44.52	44.53	44.53	44.53	44.53	0.001
0.6	38.45	38.45	38.45	38.45	38.45	0.001
0.7	34.12	34.11	34.12	34.12	34.12	0.001
0.8	30.87	30.86	30.87	30.86	30.86	0.003
0.9	28.33	28.32	28.32	28.32	28.32	0.003
1.0	26.28	26.28	26.28	26.29	26.28	0.003

Table 2. Incubation period of solid bars as a function of image coverage obtained from simulating the 100-0-0 inker for all four inking stages.

Image Coverage	Stage of Ink Feed 1	2	3	4	Mean	Standard Deviation
0.1	8.74	8.86	8.92	8.87	8.85	0.066
0.2	8.44	8.55	8.54	8.55	8.52	0.048
0.3	8.13	8.25	8.25	8.25	8.22	0.049
0.4	7.92	8.03	8.02	8.02	8.00	0.047
0.5	7.68	7.79	7.79	7.79	7.76	0.047
0.6	7.49	7.60	7.60	7.60	7.57	0.048
0.7	7.30	7.41	7.41	7.41	7.39	0.048
0.8	7.15	7.27	7.26	7.27	7.24	0.049
0.9	7.03	7.14	7.14	7.14	7.11	0.050
1.0	6.93	7.04	7.03	7.03	7.01	0.045

coverage, and the incubation period decreases with increasing image coverage. Similar results were also obtained from the halftone bars as well as from the 60-20-20 inker. Table 3 lists the mean incubation periods of solid and halftone bars as a function of image coverage for both inkers. The corresponding press time constants are summarized in Tables 4 to 7.

Table 3 data show that in all of the four cases the incubation period decreases with increasing image coverage, indicating that the incubation period can be reduced by

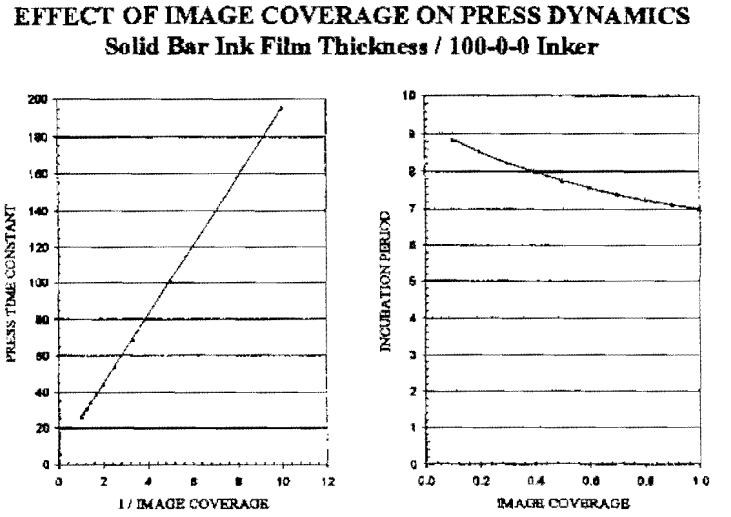

Figure 12. Effect of image coverage on dynamic behavior of the 100-0-0 inker obtained from the simulation of solid bars.

increasing the throughput rate of ink. The incubation period of the 60-20-20 inker is shorter than that of the 100-0-0 inker, consistent with the theoretical values of 2.49 versus 2.81. This phenomenon can be ascribed to the multiple ink delivery paths to the plate in the former inker as compared with the single path in the latter. One of those provides the shortest path to the web The incubation period of halftone bars is slightly longer than the corresponding solid bars for both inkers, and the difference may not be significant.

Table 3. Effect of image coverage on incubation period.

Image Coverage	100-0-0 Inker		60-20-20 Inker	
	Solid	Halftone	Solid	Halftone
0.1	8.85	9.26	5.04	5.46
0.2	8.52	8.87	4.94	5.33
0.3	8.22	8.53	4.88	5.22
0.4	8.00	8.23	4.82	5.11
0.5	7.76	7.96	4.78	5.02
0.6	7.57	7.73	4.75	4.94
0.7	7.39	7.53	4.73	4.87
0.8	7.24	7.34	4.71	4.81
0.9	7.11	7.17	4.70	4.75
1.0	7.01	7.01	4.70	4.70

Table 4. Mean press time constant of the 100-0-0 inker as a function of image coverage for solid bars.

Image Coverage	IFT	Web	F1	F2	F3	Inker Volume
0.1	195.65	195.65	189.24	195.56	195.58	194.56
0.2	100.68	100.68	95.88	100.60	100.61	99.85
0.3	69.40	69.40	64.57	69.32	69.33	68.56
0.4	53.84	53.84	48.86	53.75	53.75	52.96
0.5	44.53	44.52	39.55	44.44	44.44	43.63
0.6	38.45	38.45	33.56	38.36	38.36	37.53
0.7	34.12	34.12	29.35	34.02	34.01	33.17
0.8	30.86	30.86	26.24	30.77	30.77	29.91
0.9	28.32	28.32	23.83	28.23	28.22	27.36
1.0	26.28	26.28	21.92	26.17	26.17	25.31
R^2	0.99996	0.99996	0.99996	0.99996	0.99996	0.99997

Table 5. Mean press time constant of the 60-20-20 inker as a function of image coverage for solid bars.

Image Coverage	IFT	Web	F1	F2	F3	Inker Volume
0.1	192.15	192.15	190.54	191.72	192.13	191.88
0.2	97.35	97.35	96.04	97.00	97.33	97.13
0.3	65.99	65.99	64.56	65.56	65.96	65.76
0.4	50.28	50.28	48.69	49.78	50.24	50.02
0.5	40.94	40.94	39.21	40.37	40.91	40.66
0.6	34.83	34.83	33.00	34.17	34.78	34.54
0.7	30.49	30.49	28.58	29.74	30.45	30.18
0.8	27.22	27.22	25.23	26.40	27.18	26.89
0.9	24.66	24.66	22.61	23.77	24.61	24.31
1.0	22.61	22.60	20.52	21.65	22.54	22.25
R^2	0.99998	0.99999	1.00000	1.00000	0.99998	0.99998

addition to the dynamac behavior of printed ink film thickness, it was also found that the rates of ink flounng to the web and through each of the three ink form rollers, and the quantity of ink volume built up in the inker could all be expressed very well by equations similar to Eq. (5). Moreover, the press time constants and incubation periods of all the four stages are again the same for each image coverage. The mean press time

Table 6. Mean press time constant of the 100-0-0 inker as a function of image coverage for halftone bars.

Image Coverage	IFT	Web	F1	F2	F3	Inker Volume
0.1	196.86	196.86	190.33	196.79	196.81	195.78
0.2	101.56	101.56	96.69	101.49	101.49	100.74
0.3	69.96	69.96	65.16	69.88	69.89	69.14
0.4	54.25	54.25	49.39	54.17	54.17	53.39
0.5	44.88	44.88	40.00	44.79	44.79	43.98
0.6	38.65	38.65	33.82	38.55	38.55	37.73
0.7	34.21	34.21	29.48	34.11	34.11	33.28
0.8	30.90	30.90	26.28	30.81	30.79	29.95
0.9	28.33	28.33	23.84	28.24	28.22	27.37
1.0	26.28	26.28	21.92	26.17	26.17	25.31
R^2	0.99998	0.99998	0.99998	0.99998	0.99998	0.99999

Table 7. Mean press time constant of the 60-20-20 inker as a function of image coverage for halftone bars.

Image Coverage	IFT	Web	F1	F2	F3	Inker Volume
0.1	193.28	193.28	191.64	192.92	193.26	193.01
0.2	98.15	98.15	96.82	97.82	98.13	97.93
0.3	66.52	66.52	65.09	66.12	66.49	66.29
0.4	50.76	50.76	49.18	50.27	50.72	50.50
0.5	41.33	41.33	39.62	40.75	41.29	41.04
0.6	35.06	35.06	33.24	34.40	35.00	34.76
0.7	30.60	30.60	28.69	29.86	30.54	30.28
0.8	27.26	27.26	25.27	26.44	27.22	26.93
0.9	24.67	24.67	22.63	23.78	24.62	24.33
1.0	22.61	22.60	20.52	21.65	22.54	22.25
R^2	0.99999	0.99999	1.00000	1.00000	0.99999	1.00000

constants obtained from the solid bars are listed in Tables 4 and 5 for the 100-0-0 and 60-20-20 inkers, respectively. In those tables the abbreviation "IFT" represents the printed ink film thickness; "Web", "F1", "F2", and "F3" stand for the rates of ink flow to the web and through ink form roller #1, #2, and #3, respectively. "Inker Volume" represents the quantity of ink volume built up in the inker. Linear regression

coefficients, R^2, are included to illustrate the relationship between press time constant and reciprocal image coverage. The mean press time constants obtained from the halftone bars are listed in Tables 6 and 7 for the 100-0-0 and 60-20-20 inkers, respectively. Perfect linear relationships between press time constant and reciprocal image coverage-are obtained for all of the properties investigated in the simulation.

Data in Tables 4 to 7 show that the press time constant obtained from the printed ink film thickness (in the IFT column) is slightly smaller for the 60-20-20 inker than for the 100-0-0 inker. That is, the former inker tends to respond to a change in ink feedrate faster than the latter. This can also be ascribed to the fact that the 60-20-20 inker has multiple ink delivery paths to the plate and the 100-0-0 inker practically, has only one path. The press time constant of halftone bars is slightly larger than the corresponding solid bars for both inkers, and the difference is not significant. These phenomena are similar to those of incubation period. The tentative conclusions are that the 60-20-20 inker tends to respond to an ink feedrate change faster than the 100-0-0 inker does, and the higher the image coverage, the faster the press response. The effect of image constitution, solid or halftone image, appears insignificant.

Close examination of Tables 4 to 7 also reveals that for the 100-0-0 inker the press time constant obtained from the rate of ink flowing through the first form roller is smaller than those of the second and third forms, and the latter two constants are almost identical. As for the 60-20-20 inker, the press time constant obtained from the ink flow rate through the first form roller is slightly smaller than that of the second one, which is in turn slightly smaller than that of the third. These and aforementioned results are consistent with the ink flow ratios discussed in a previous section. They indicate that the press time constant and incubation period both can be remarkably reduced if the throughout rate of ink is increased correspondingly. Such inkers shall reduce tremendously the waste from makeready and any change in press conditions. This concept has been applied to designing novel printing presses for waterless lithography (Chou, et al., 1996).

All of the simulation results presented so far have led to a common conclusion that both press time constant and incubation period are independent of any change in ink feedrate, regardless of the direction and magnitude of the change. This finding appears to contradict results reported in the literature. Chung and Chung (1992) found that a small change in ink feedrate took longer to reach the equilibrium than a large change. Neuman and Almendinger (1977) observed that a decrease of the ink feed generally produced a longer press time constant than did a corresponding increase. It is possible that the electronic and/or mechanical delay in responding to a stop increase in ink feedrate may be different from that of a step decrease. However, close inspection of the test conditions of those works indicates that the tools used to monitor output changes are different. Densitometry or colorimetry was used by Chung and Chung (1992) and Neuman and Almendinger (1977) to monitor the printed output, whereas changes in the printed ink film thickness were calculated in the present study. Besides, there is no electronic and/or mechanical delay in the simulation.

It can be proven mathematically that the response time needed for a press to reach a steady state due to a change in ink feedrate is independent of the magnitude and the direction of change, as long as the split ratios remain constant throughout the entire distribution process. So, the discrepancy between these theoretical predictions and previously mentioned experimental works may very well come from the non-linear relationship between optical density and ink film thickness, which is a well-known fact and is generally referred to as ink mileage curve. Several models had been proposed to relate optical density to ink film thickness. Chou and Harbin (1991) found that the best model was proposed by Calabro and Savagnone (1983) as follows.

$$\frac{1}{D} = \frac{1}{D_S} + \left(\frac{m}{H}\right)^n \tag{6}$$

where D and H represent optical density and ink film thickness, respectively. The parameter D_S is the saturation density which is the density at infinite ink film thickness or the maximum density that can be achieved by the ink. The parameter m is generally referred to as density smoothness which characterizes how fast the ink mileage curve approaches the saturation density. The exponent n is a power law index generally implemented to improve the fitness of equation to experimental data.

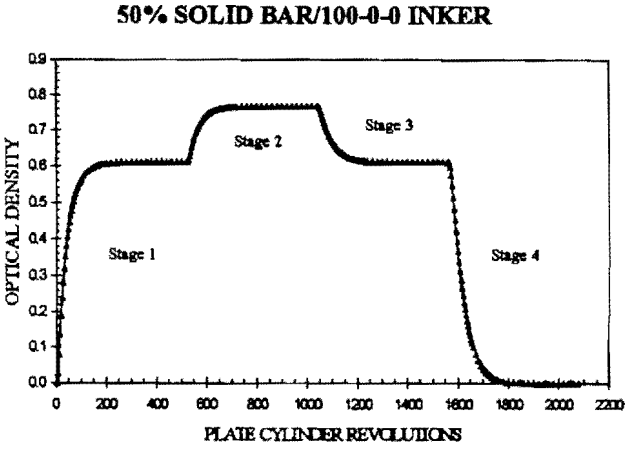

Figure 13. Dynamic behavior of optical density of the 50% solid bar. Density data were converted from the printed ink film thickness data in Figure 10.

Using the parameters of D_S = 1.39, m = 0.914, and n = 1.095 reported for the master curve of a magenta ink (Chou and Harbin, 1991) to convert ink film thickness into optical density, Figure 10 data are replotted in Figure 13. The data in both figures have a similar trend. The following equation, a clone of Eq. (5), is used to describe the

Table 8. Incubation period obtained from the analysis of optical densiity as a function of image coverage for the 100-0-0 inker.

Enage	Solid Bar				Haltone Bar			
Coverage	0-1μ	1-0μ	1-1.5μ	1.5-1μ	0-1μ	1-0μ	1-1.5μ	1.5-1μ
0.1	7.59	15.23	6.48	10.53	12.36	9.86	9.23	9.48
0.2	6.64	14.89	6.91	10.48	10.19	10.00	8.52	9.32
0.3	6.55	13.45	6.94	9.87	8.98	9.95	8.05	9.13
0.4	6.53	12.35	6.93	9.40	8.20	9.85	7.69	8.91
0.5	6.47	11.42	6.83	8.98	7.67	9.71	7.39	8.70
0.6	6.37	10.82	6.76	8.63	7.21	9.62	7.15	8.47
0.7	6.26	10.34	6.62	8.38	6.84	9.55	6.90	8.31
0.8	6.17	9.95	6.55	8.14	6.55	9.49	6.73	8.11
0.9	6.09	9.66	6.46	7.98	6.28	9.45	6.55	7.98
1.0	6.02	9.41	6.40	7.82	6.02	9.41	6.40	7.82

Table9. Incubation period obtained from the analysis of optical density as a function of image coverage for the 60-20-20 inker.

Image	Solid Bar				Halitone Bar			
Coverage	0-1μ	1-0μ	1-1.5μ	1.5-1μ	0-1μ	1-0μ	1-1.5μ	1.5-1μ
0.1	3.78	11.43	2.90	6.69	8.49	6.08	5.41	5.65
0.2	3.17	11.13	3.45	6.83	6.56	6.44	4.99	5.77
0.3	3.38	9.80	3.74	6.41	5.61	6.57	4.79	5.78
0.4	3.57	8.79	3.90	6.07	5.08	6.60	4.65	5.73
0.5	3.72	8.03	3.99	5.84	4.77	6.58	4.55	5.66
0.6	3.80	7.58	4.09	5.65	4.53	6.60	4.48	5.57
0.7	3.86	7.25	4.12	5.56	4.35	6.60	4.40	5.53
0.8	3.90	6.98	4.17	5.45	4.20	6.61	4.35	5.45
0.9	3.94	6.79	4.20	5.40	4.07	6.62	4.28	5.40
1.0	3.96	6.64	4.24	5.33	3.96	6.64	4.24	5.33

dynamic response of optical density.

$$D = D_O + (D_\infty - D_O)\left[1 - \exp[-(N - N_d)/\tau_p]\right] \tag{7}$$

where D represents optical density. The other terms are identical to those defined in Eq. (5). Figure 13 shows that Eq. (7) fits the data very well, from which parameters

Table 10. Press time constant obtained from the analysis of optical density as a function of image coverage for the 100-0-0 inker.

Image	Solid Bar				Halftone Bar			
Coverage	0-1μ	1-0μ	1-1.5μ	1.5-1μ	0-1μ	1-0μ	1-1.5μ	1.5-1μ
0.1	137.69	306.50	166.23	225.13	203.38	188.63	192.91	198.56
0.2	76.24	126.71	89.74	112.64	99.29	99.56	98.86	104.15
0.3	53.77	83.20	62.67	76.53	66.28	70.20	67.37	72.55
0.4	42.16	63.42	48.88	59.00	49.98	55.72	51.73	56.79
0.5	35.27	51.81	40.53	48.67	40.37	47.00	42.41	47.36
0.6	30.58	44.53	3S.19	41.82	33.92	41.32	36.33	40.99
0.7	27.23	39.37	31.18	37.13	29.33	37.29	31.89	36.59
0.8	24.70	35.52	28.31	33.48	25.89	34.29	28.68	33.17
0.9	22.73	32.51	25.95	30.74	23.24	31.96	26.11	30.60
1.0	21.14	30.10	24.15	28.44	21.14	30.10	24.15	28.44
R^2	0.9991	0.9893	0.9997	0.9996	0.9997	0.9999	1.0000	1.0000

Table 11. Press time constant obtained from the analysis of optical density as a function of image coverage for the 60-20-20 inker.

Image	Solid Bar				Halftone Bar			
Coverage	0-1μ	1-0μ	1-1.5μ	1.5-1μ	0-1μ	1-0μ	1-1.5μ	1.5-1μ
0.1	135.55	298.06	163.54	220.93	199.60	185.08	189.60	194.88
0.2	73.71	122.04	86.80	108.85	96.03	96.12	95.57	100.65
0.3	50.97	79.11	59.51	72.81	63.05	66.72	64.03	69.00
0.4	39.15	59.38	45.54	55.20	46.73	52.15	48.34	53.17
0.5	32.19	47.84	37.15	44.86	37.11	43.35	38.98	43.68
0.6	27.45	40.56	31.75	38.00	30.64	37.59	32.86	37.27
0.7	24.09	35.43	27.75	33.31	26.06	33.49	28.40	32.81
0.8	21.54	31.57	24.85	29.64	22.65	30.42	25.19	29.35
0.9	19.S5	28.5S	22.48	26.88	20.04	28.04	22.62	26.75
1.0	17.96	26.13	20.67	24.59	17.96	26.13	20.67	24.S9
R^2	0.9990	0.9901	0.9996	0.9997	0.9997	1.0000	1.0000	1.0000

characterizing the press dynamics can be derived. Tables 8 to 11 summarize the incubation periods and press time constants as a function of image coverage for solid and halftone bars obtained from simulating the 100-0-0 and 60-20-20 inkers, respectively. These tables demonstrate clearly that as the optical density is used as a

control means, both incubation period and press time constant vary with the magnitude and direction of ink feedrate change.

The data in Tables 8 to 11 indicate that both incubation period and press time constant for a step increase (0-1μ and 1-1.5μ, or stages 1 and 3) are indeed smaller than those for a stop decrease (1-0μ and 1.5-1μ, or stages 2 and 4) at any image coverage for both inkers. Moreover, the press time constant for a small change in ink feedrate (1-1.5μ) is larger than that for a large change (0-1μ). So, the apparent discrepancy between theoretical predictions and experimental data comes primarily from the non-linear relationship between optical density and ink film thickness. It becomes clear that as the densitometry is used as a control means, the press time constant is closely relatod to the slope of ink mileage curve at the initial point. The press response time to a small inking change may not be necessarily longer than that of a large inking change. For example, the press time constant for a step increase of 0-0.5μ is predictod to be smaller than that of 0.5-1.5μ step increase. Tables 10 and 11 data also indicate that the press time constant derived from optical density measurements is inversely proportional to the image coverage, as evidenced by the linear regression coefficient, R^2.

Mean Ink Residence Time

MacPhee, et al. (1986) proposed a Markov-chain model to simulate the printing process in that the mean ink passage time from any roller to paper was calculated. They also proposed an inventory-throughput model that defined the mean ink residence time as the ratio of the ink volume in the inker to the ink throughput or feedrate. The mean ink residence times calculated by both models agree with each other very well. They found that when the image coverage decreases to less than 10%, mean ink

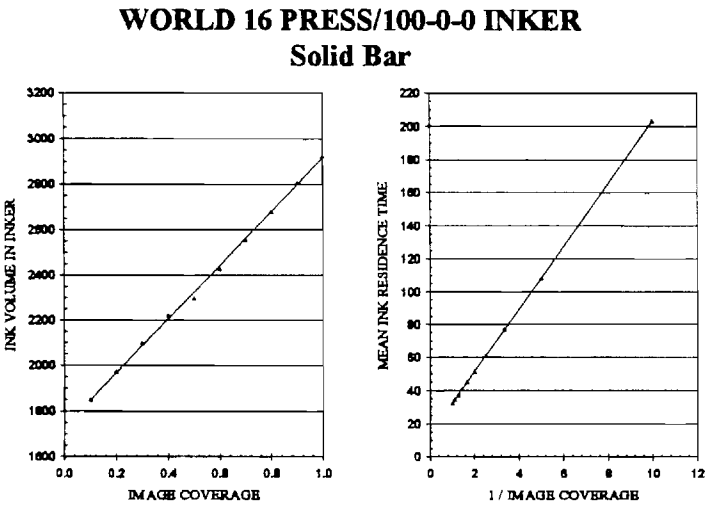

Figure 14. Relationships of ink volume in the 100-0-0 inker and mean ink residence time with the image coverage.

residence time increases rapidly. In fact, it was found by using a typical linear regression program, such as Lotus 123, to analyze their data that the mean ink residence time is inversely proportional to the image coverage.

It is relatively simple to calculate the ink volume in the inker and hence the mean ink residence time using the computer simulation program reported here. The example in Figure 14 illustrates that the ink volume in the inker is proportional to and the mean ink residence time is inversely proportional to the image coverage. Table 12 lists the calculated ink volume and mean ink residence time of solid and halftone bars for the 100-0-0 and 60-20-20 inkers as a function of image coverage. The linear regression coefficients, W, listed in the table again support the claim that the ink volume in the inker is proportional to and the mean ink residence time is inversely proportional to the image coverage. MacPhee (1995) pointed out that the mean ink residence time provided an upper limit estimate of the press time constant. The same conclusion is obtained from comparing the data in Table 12 to the data in Tables 4 to 7.

Table 12. Ink volumes in the inker (Ink V.) and mean ink residence times (Res. T.) of the solid and halftone bars for the 100-0-0 and 60-20-20 inkers.

Image Coverage	100-0-0 Inker				60-20-20 Inker			
	Solid Bar		Halftone Bar		Solid Bar		Halftone Bar	
	Ink V.	Res. T.	Ink V.	Res. T.	Ink V.	Res. T.	Ink V.	Res. T.
0.1	1849.7	203.27	1864.5	204.89	1788.4	196.53	1802.5	198.08
0.2	1971.6	108.33	1993.9	109.55	1851.3	101.72	1872.9	102.91
0.3	2096.8	76.81	2120.7	77.68	1919.4	70.31	1943.1	71.18
0.4	2221.7	61.03	2245.1	61.68	1985.4	54.54	2013.2	55.31
0.5	2295.6	51.48	2320.1	52.03	2013.5	45.16	2041.5	45.78
0.6	2427.4	45.21	2446.4	45.57	2094.7	39.01	2117.0	39.43
0.7	2554.5	40.68	2569.4	40.92	2175.6	34.65	2190.9	34.89
0.8	2680.1	37.28	2689.8	37.42	2253.7	31.35	2263.5	31.49
0.9	2803.2	34.61	2808.1	34.67	2330.6	28.78	2335.4	28.84
1.0	2924.6	32.46	2924.6	32.46	2406.8	26.72	2406.8	26.72
R^2	0.9987	1.0000	0.9989	1.0000	0.9936	1.0000	0.9964	1.0000

Applications To Printing Process Control

It has been demonstrated in the industry that a printing press can produce a stable, consistent result once the ink fountain keys are set and the press is left alone without any disturbance. However, in the real world the pressman usually use a densitometer to measure optical density of a color control bar to monitor the printing process. If the

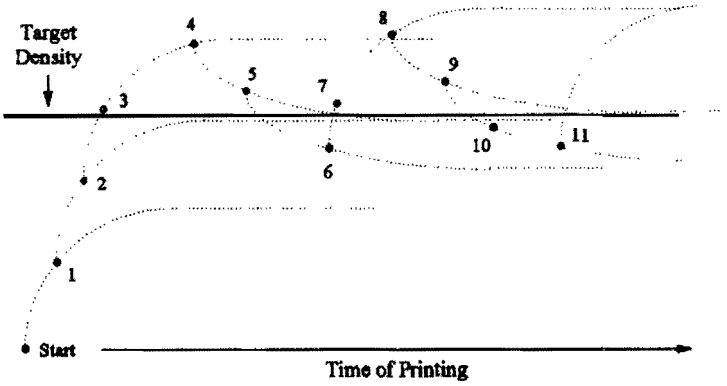

Figure 15. Schematic diagram illustrating the common phenomenon of chasing after the target density usually happened in a pressroom. The dotted curves characterize the dynamic response of the press to a change in ink feedrate.

optical density is lower than the target value, the ink feedrate is increased and another sample is subsequently taken and measured. If the target density is not achieved, the ink feedrate is increased again. In many cases the pressmen do not wait long enough before taking a sample for optical density measurement, and than make unnecessary adjustments. Soon they will find out that the optical density is too high and immediately reduce the ink feedrate. Thus, the pressmen are always chasing after the target density and the process is fluctuating around the target density throughout the entire printing process, as is shown schematically in Figure 15.

To keep away from the trap of chasing after the target density, one must know, first of all, the image coverage of each inking zone corresponding to the color control bar, because the press time constant is inversely proportional to the image coverage. Secondly, because a densitometer is commonly used in the pressroom to control the printing process, it has to be kept in mind that it takes longer for the press to reach the steady state by reducing the ink feedrate than increasing it. Always allow sufficient time for the press to respond to any change in ink feedrate. A wise recommendation is never to overfeed the ink. This will minimize waste resulting from ink feedrate change. It may not be easy for a pressman to follow the rules of using a densitometer to control the printing process. However, Eqs. (5) and (6) can be built in the closed-loop control algorithm to monitor the printing process precisely.

Conclusions

The results of this computer simulation are consistent with those of other simulation programs. They also agree with experimental results reported in the literature.

The 100-0-0 inker tends to produce an ink film more uniform than the 60-20-20 inker does. This is ascribed to the second and third ink form rollers whose major function is to smooth out the ink film laid down on the plate by the first form roller. The dynamic response to a step change in ink feedrate is faster for the 60-20-20 inker than the 100-0-0 inker, due to multiple ink delivery paths of the former compared to the single path of the latter. Each inker configuration apparently has its own advantages. Selection of an inker may depend on personal preference.

If the ink film thickness is used as the control variable, the dynamic behavior of a press is independent of the magnitude and direction of a step change in ink feedrate. That is, both press time constant and incubation period are not affected by the change in ink feedrate. If the optical density is used as the control variable, the press responds to a step increase in ink feedrate faster than a step decrease and, in some cases, the response to a large change may be faster than a small one. Differences in the dynamic behavior predominantly result from the non-linear relationship between optical density and ink film thickness.

The results of press dynamics in the printed ink film thickness, rates of ink flowing to the web and through each of the three ink form rollers, the quantity of ink volume built up in the inker, and the mean ink residence time all indicate that the press time constant is inversely proportional to the image coverage. This is very important to the control of printing process, as many pressmen may not give the system enough time to reach the steady state and keep changing ink feedrate constantly. Excessive waste may result from this practice of chasing after the target density.

Acknowledgments

The authors would like to acknowledge Ms. Mariam Vahabi who initiated the computer simulation program and laid down a solid foundation for them to resume this project.

Reference Cited

Calabro, G. and Savagnone, F.
1983 "A Method for Evaluating Printability," Adv. Printing Sci. Tech., Vol. 17, pp. 358-380.

Chou, S. M., Bain, L. J., Durand, R., and Sanderson, E.
1996 "A Novel Printing Press for Waterless Lithography'" to be presented at the International Printing and Graphic Arts Conference in Minneapolis, September 16-19, sponsored by TAPPI and CPPA.

Chou, S. M. and Harbin, N.
1991 Relationship Between Ink Mileage and Ink Transfer." TAGA Proceedings, pp. 405-432.

Chung, R. and Chung S. D.
1992 "An Investigation of Press Response Time Due to Inking Change on a Web Offset Press." TAGA Proceedings, pp. 527-535.

Guerrette, D. J.
1985 "A Steady State Inking System Model for Predicting Ink Film Thickness Distribution," TAGA Proceedings, pp. 404-425.

Hull, HH.
1968 "The Theoretical Analysis and Practical Evaluation of Roller Ink Distribution Systems." TAGA Proceedings, pp. 288-315.

MacPhee, J.
1995 "A Relatively Simple Method for Calculating the Dynamic Behavior of Inking Systems, "TAGA Proceedings, pp. 168-183.

MacPhee, J., Kolesar, P., and Federgun, A.
1986 "Relationship Between Ink Coverage and Mean Ink Residence Time in the Roller Train of a Printing Press," Adv. Printing Sci. Tech., Vol. 18, pp. 297-317.

Mill, C. C.
1961 "An Experimental Test of a Theory of Ink Distribution," Adv. Printing Sci. Tech, Vol. 1, pp. 183-197.

Neuman C. P. and Almendinger, F. J.
1977 "Experimental Model Building of the Lithographic Printing Process II," GATF Annual Research Department Report, pp. 23-47.

Neuman C. P. and Almendinger, F. J.
1978 "Experimental Model Building of the Lithographic Panting Process III" GATF Annual Research Department Report, pp. 181-207.

Scheuter, K. R. and Rech, H.
1970 "About Measurement and Computation of Ink Transfer in Roller Inking Units of Printing Presses," TAGA Proceedings, pp. 70-87.

Wirz, B.
1964 "Studies on Inkers for Letterpress and Lithographic Rotary Presses," TAGA Proceedings, pp. 102-117.